JOURNAL OF MATERIALS SCIENCE 29 (1994) 5593–5598

Growth parameter effect in superconducting $YBa_2Cu_4O_8$ thin films by d.c. magnetron sputtering

S. C. WU, H. T. HSU, F. H. CHEN, W. R. CHANG, T. Y. TSENG
Department of Electronics Engineering and Institute of Electronics, National Chiao-Tung University, Hsinchu, Taiwan

High-T_c $YBa_2Cu_4O_8$ (124) thin films have been made by d.c. magnetron sputtering deposition on (1 0 0) MgO substrates. The effect of several processing variables, including the ratio of oxygen to argon, total pressure, and substrate temperature, on the superconducting properties of the thin films, were systematically investigated. The as-prepared films annealed in flowing oxygen at 800 °C for 4 h under ambient pressure obtained nearly phase-pure 124 and exhibited superconducting onset transition at 75 K.

1. Introduction

The crystal structure of "124" phase ($YBa_2Cu_4O_8$) differs from that of "123" phase ($YBa_2Cu_3O_{7-x}$) in that the single Cu–O chain has been replaced by a double chain [1], and that it exhibits a T_c (zero) about 75–80 K (or 90 K if doped with calcium [2]) compared to the 123 superconductor with T_c near 93 K. The high stability of the oxygen content in 124 with respect to 123 by the double-chain effect, offers more advantages for important applications, e.g. metal-clad composite wire. On the other hand, the double chains also cause the crystal structure to become less orthorhombic; the orthorhombicities of 124 and 123 are 0.8% and 1.8%, respectively [3]. The lower degree of orthorhombicity, and less frequent appearance of twin structure during phase transformation in annealing, improves the surface quality of the thin film.

The 124 phase was first observed as a lattice defect in partially decomposed 123 powders [4], and then as an ordered defect structure in the 123 thin film [5, 6]. Immediately, 124 superconductor was prepared as the main phase in epitaxial thin film [7]; subsequently, the bulk form of 124 phase was synthesized by Karpinski *et al.* [8].

Fabrication of thin crystalline forms of $YBa_2Cu_4O_8$ was made by r.f. sputtering [9], evaporation [6], molecular beam epitaxy [7], laser ablation [10] and metal organic chemical vapour deposition [11]. However, the formation of 124 YBCO superconducting thin film by d.c. single-target sputtering has not so far been reported. In the present work, we investigated the dependence of the composition of as-deposited film on total pressure, output sputtering current, oxygen ratio and substrate temperature. It was found that it was possible to form a film containing 124 majority phase after post-annealing at 800 °C, by controlling the sputtering conditions.

2. Experimental procedure

$YBa_2Cu_4O_8$ thin films were deposited on MgO (1 0 0) substrate by d.c. magnetron sputtering with a single target. The $YBa_2Cu_4O_8$ target was fabricated using a mixture of Y_2O_3, $BaCO_3$ and CuO powders, which was prepared in stoichiometric composition. The powders were mixed using alcohol as a medium with a wet-ball mill, dried using an infrared lamp, calcined repeatedly several times at 890 °C for 10 h for homogenization, and ground to sieve through 325 mesh, then cold pressed into 50 mm diameter discs. The discs were sintered at 900 °C for 8 h in static air. Target was presputtered for 20 h prior to initiating film-growth experiments in a vacuum chamber.

To investigate the variation of the composition of thin film with growth conditions, deposition processes were performed in a glow discharge at a total pressure equal to 50–600 mtorr (1 torr = 133.322 Pa), and a d.c. sputtering current in the range 24–192 mA. The sputtering gas was a mixture of argon and oxygen, such that the ratio of oxygen to argon was between 0% and 60%. The target-to-substrate distance was 40 mm. The substrate temperature was varied from room temperature to 600 °C. After deposition, the substrate heater was turned off and pure oxygen was immediately introduced into chamber. The films were cooled to 150–200 °C in about 25 min before removing the samples from the chamber. The subsequent annealing processes were kept at 650 °C for 1 h, then at 750 °C for 1 h and finally at 800 °C for 1 h, then cooled to room temperature. The annealing atmosphere was flowing dry oxygen. The heating and cooling rates were 10 and 2 °C min^{-1}, respectively.

The composition of metallic elements in the films was analysed by inductively coupled plasma emission spectroscopy (ICP). The crystal structure of the films was examined by X-ray diffraction (XRD) measurement using a CuK_α source at 40 kV, 20 mA. The

0022–2461

surface morphology was observed by scanning electron microscopy (SEM), and the electrical resistivity was measured by a standard four-point probe method.

3. Results and discussion

Fig. 1 shows the dependence of Cu/Y and Ba/Y atomic ratios of the film on the total chamber pressure. It is indicated that the Cu/Y and Ba/Y atomic ratios in the films exhibit a continuously increasing trend with increasing total pressure when the composition of the target was kept at 1:2:4 (Y:Ba:Cu). The modes of transportation of sputtered particles may be divided into three types depending on chamber pressure. The transport of particles which were sputtered by argon ions is diffusive and is characterized by simple gas-phase diffusion at high pressure [12]. At low pressure, the transport is ballistic, and the sputtered atoms have virtually no collisions with gas atoms during transport. At intermediate pressure, the form of transport is more complicated between the case of high and low pressures. In this regime, the lighter sputtered species tended to suffer more momentum and direction-changing collisions than the heavier atoms [13]. However, the threshold pressure for effective scattering is uncertain, owing to the initial high energy of sputtered atoms. Several mean free paths are necessary to thermalize a sputtered atom for diffusive transport [12]. The deposition rate, R, is proportional to the target sputtering rate, S, and the mean free path, h, for diffusion, but is inversely proportional to the target–substrate distance, L, given by [12]

$$R = \frac{4Sh}{3L} \tag{1}$$

because h varies with $1/p$, where p is the total pressure. Therefore, increasing the total pressure will reduce the deposition rate of all metal atoms or ions. In particular, the reduction rate of yttrium species is the most serious of the three, from our experimental data (Fig. 1). In the diffusion process, the dominant factor is the scattering of particles that determines the value of the mean free path. The scattering effect is dependent on particle energy, mass, atomic number of atoms involved, even the valence value of the sputtered atom [14]. The target sputtering rate, S, is not only relative to the items mentioned above, but also is a function of the incident argon ion energy and the surface binding energy of the target [15]

$$S = \frac{3\alpha}{4\pi^2} \frac{4m_i m_t}{(m_i + m_t)^2} \frac{E}{U_o} \tag{2}$$

For yttrium atoms, the binding energy with oxygen is the highest of the three metallic elements, about three times and ten times higher than that of barium and copper, respectively. The valence value of yttrium is 3, but those of barium and copper are both 2. Substituting equation 2 into equation 1, the deposition rate, R, can therefore be expressed as

$$R = \frac{h\alpha}{\pi^2 L} \frac{4m_i m_t}{(m_i + m_t)^2} \frac{E}{U_o} \tag{3}$$

where U_o is the surface binding energy of the material being sputtered, E is the output power during sputtering, and α is a monotonically increasing function of m_t/m_i which has value of 0.17 for $m_t/m_i = 0.1$, increasing up to 1.4 for $m_t/m_i = 10$, m_t and m_i are the masses of target atom and incident ion, respectively [15]. In our case, m_t/m_i is about 3.4 for barium, 2.2 for yttrium, and 1.6 for copper, thus, α is about the same. The difference in U_o, which has been mentioned above, is a vital factor.

The deposition rates of copper, barium and yttrium atoms can be calculated on the basis of Equation 3 by using the parameters summarized in Table I.

$$R_{Cu} = \left(\frac{4h}{\pi^2 L}\right) E \left(\frac{0.4}{u_{Cu}}\right) \tag{4}$$

$$R_{Ba} = \left(\frac{4h}{\pi^2 L}\right) E \left(\frac{0.4}{u_{Ba}}\right) \tag{5}$$

and

$$R_Y = \left(\frac{4h}{\pi^2 L}\right) E \left(\frac{0.4}{u_Y}\right) \tag{6}$$

Because the composition of the target is Y:Ba:Cu = 1:2:4, the deposition rate of copper and barium must multiply by factors 4 and 2, respectively. In addition, from the kinetic gas theory, the mean free path, h, of the sputtering atom with mass m_S, travelling through a gas consisting of atoms of mass m_g is represented by [14]

$$h^{-1} = 1.11 \times 10^{14} \frac{(r_S + r_g)^2}{4} (1 + m_S/m_g)^{1/2} P \tag{7}$$

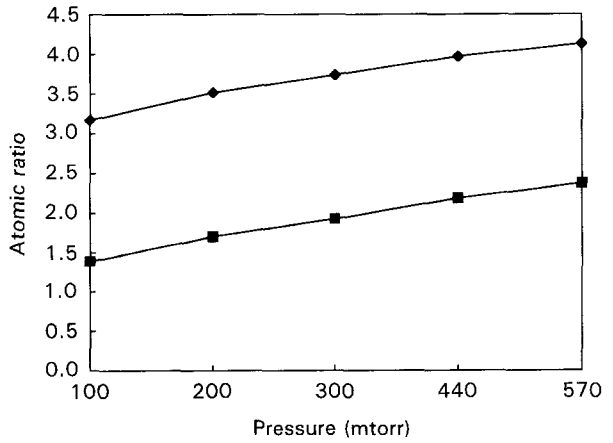

Figure 1 Dependence of the atom ratios of (◆) Cu/Y and (■) Ba/Y on the total chamber pressure. The target composition was Y:Ba:Cu = 1:2:4.

TABLE I Physical parameters of the atoms sputtered[a]

	M(g) Mass of atom	r(nm) Radius of atom	U(kcal mol^{-1} Binding energy with oxygen
Cu	64	0.19	41
Ba	137	0.29	136
Y	89	0.274	420
Ar	40	0.19	

[a]data from a published data book

where r_S and r_g are the radii of sputtered atom and gas atom, respectively, and P is the chamber pressure.

The atomic ratios of copper to yttrium ($R_{Cu/Y}$) and barium to yttrium ($R_{Ba/Y}$) are equal to 62 and 5.8, respectively, on the basis of Equations 4–7. These calculated values of the ratios of copper to yttrium and barium to yttrium deviate significantly from the experimental data. Therefore, there must be some factors which have not yet been considered which have an influence on the results. These factors may be the sticking coefficiency, the valence number, the resputtering effect by the negative ion and the interaction between these factors. The sticking coefficiency of each sputtered atom in a compound target is not well known, therefore, all researchers in the sputtering field always set its value as unity. The effect of negative ion resputtering is often observed on sputtering of oxides or certain intermetallic compounds [17–19], and we also found the same in our experiments, as shown in Fig. 7. If we estimate the deposition rate of each metal atom based on the considerations above, the relative values can be found, and then these can be induced into a general experimental rule on the composition of metal atoms in any growth condition. However, we cannot determine exactly the quantities of those effects. If we assume that the deposition rate depending on those effects is a function of pressure to various degrees for different atoms, it is expressed by $R = KP^{-a}$, where K and a are the factors which depend on growth conditions and kinds of sputtered atoms. Then $R_{Cu/Y}$ and $R_{Ba/Y}$ can be written as

$$R_{Cu/Y} = \frac{k_{Cu}}{k_Y} P^{(a_Y - a_{Cu})} = k_c P^c \quad (8)$$

$$R_{Ba/Y} = \frac{k_{Ba}}{k_Y} P^{(a_Y - a_{Ba})} = k_b P^b \quad (9)$$

A plot of Equations 8 and 9 by taking their natural logarithm form, is indicated in Fig. 2. The values of b and c, which can be obtained from the slopes of the straight lines on this figure, are 0.3 and 0.15, respectively. The degree of dependence of the deposition rate on pressure for the yttrium atom, is the highest of the three atoms, because $a_Y > a_{Cu} > a_{Ba}$. That is, at higher chamber pressure, the barium atom, because of its greater mass, is able to transmit the lighter gas atoms better than the others. On the other hand, owing to the large-angle scattering for the lighter atom, the $R_{Cu/Y}$ is larger in which the radial distance is further away from the center, but for $R_{Ba/Y}$ the reverse is true.

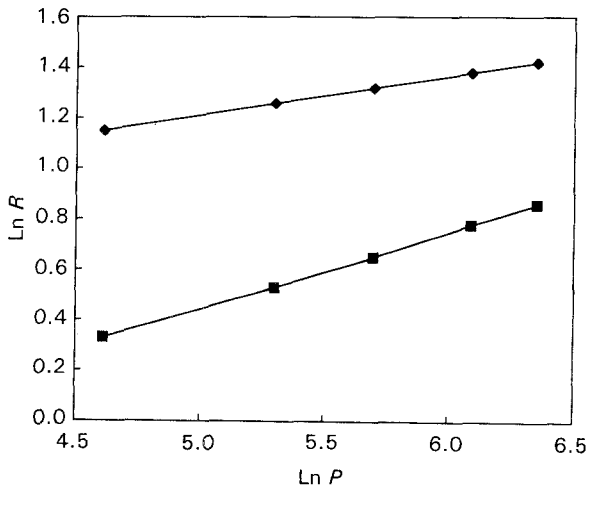

Figure 2 Natural logarithm plot of the relative deposition ratio of (◆) Cu/Y and (■) Ba/Y versus chamber pressure.

Fig. 3 shows scanning electron micrographs of the surfaces of the thin films after annealing, which were deposited at various chamber pressures. They indicate that the film surfaces contain many prominent particles. The number of prominent particles in the film surface clearly reduces with increasing pressure. One possible reason is that the sputtered atoms are more fully thermalized by the gas atom at higher pressure, which leads to greater homogenization [20].

Figs 4–6 show the dependence of $R_{Cu/Y}$ and $R_{Ba/Y}$ on the ratio of oxygen to argon, the output sputtering current and substrate temperature, respectively. The atomic ratio of Ba/Y exhibits a decreasing trend with increasing O_2/Ar ratio, as shown in Fig. 4. In particular, at zero oxygen content, the Ba/Y ratio is the largest of all. The trend of the change in Cu/Y atomic ratio exhibits a similar pattern to Ba/Y, excluding a small jump at an O_2/Ar ratio of 20/100. Back-sputtering of negative oxygen ions is the most probable factor for that behaviour. The seriously damaged film shown in Fig. 7 was produced with a high oxygen ratio (> 25%), a lower chamber pressure (< 200 mtorr) and a high output current (> 168 mA). For yttrium, the back-sputtering is not so serious, owing to the strong binding energy. But the copper component, whose vapour pressure is the highest of the three, is easily resputtered under a high oxygen content [15]. From Fig. 5, the Ba/Y ratio is seen to have less influence on sputtering current, whereas the change with the Cu/Y ratio is obvious. There are two points of view about this, the change in discharge power can induce the gas rarefaction effect, thus producing various scattering events, similar to the effect of chamber pressure, mentioned above. The local gas density, n_g, near the cathode can be found as a function of the discharge current, I [13]. The lower current produces a higher local gas density, and thus $R_{Cu/Y}$ is higher than the others. A second view is that the sputtering yield of each of the compounds may have an energy threshold value, for yttrium the threshold valve is higher than for copper, so the higher the discharge current, the greater is the yield of yttrium. The critical point, due to the counter-balancing of both effects between gas rarefaction and minimum energy threshold, is about 120 mA output current. However, the trends in the variation of the Ba/Y and Cu/Y ratios are the same. Fig. 6 shows the dependence of the Cu/Y and Ba/Y atomic ratios on the substrate temperature. Note that the Cu/Y atomic ratio changes randomly over the whole temperature range, while the Ba/Y ratio remains almost unchanged. An unchanged Ba/Y ratio was also attained by Arikawa *et al.* [16]. It has also been indicated that stoichiometric films can be achieved at temperatures of 200 and 400 °C, with the Cu/Y ratio having a minimum value at 300 °C, which probably bears some relation to the sticking

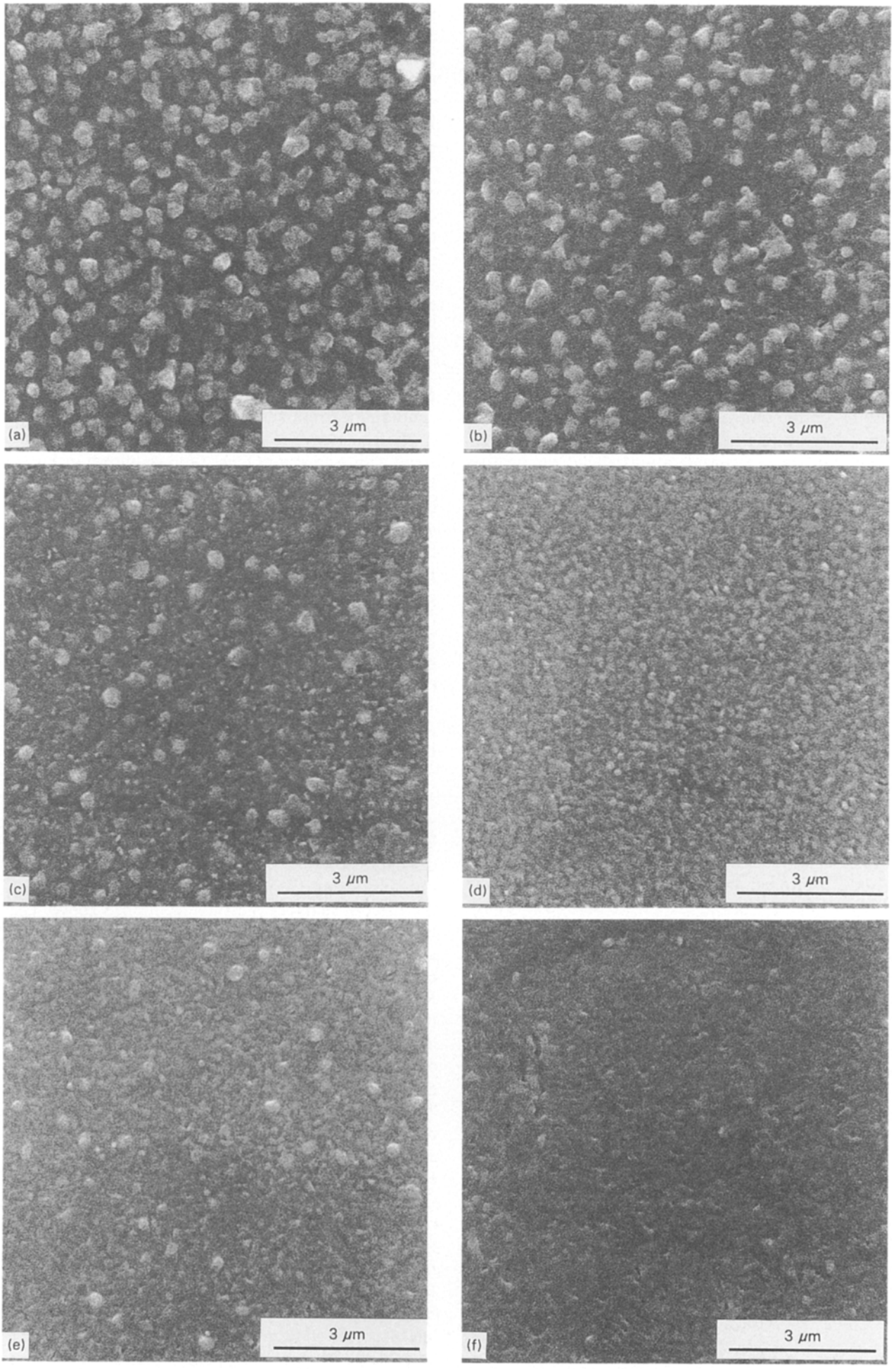

Figure 3 Scanning electron micrographs of the surface of annealed films. Films were deposited = 500 °C, O_2/Ar = 5/100, I_{out} = 48 mA, and various pressures: (a) 50 mtorr, (b) 100 mtorr, (c) 200 mtorr, (d) 300 mtorr, (e) 440 mtorr, (f) 570 mtorr.

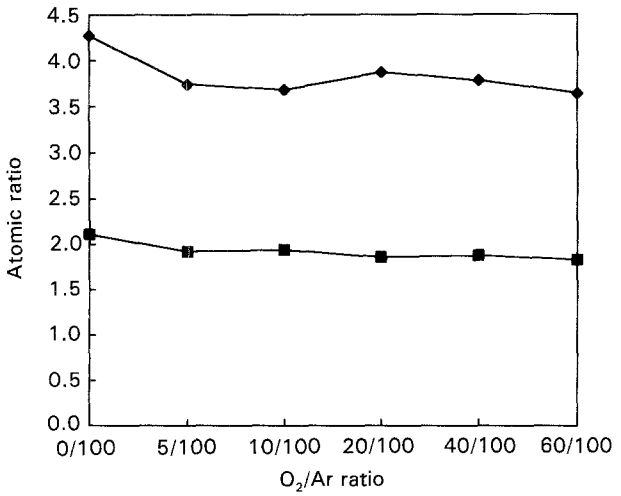

Figure 4 Dependence of atomic ratios (◆) Cu/Y and (■) Ba/Y on the O_2Ar ratio.

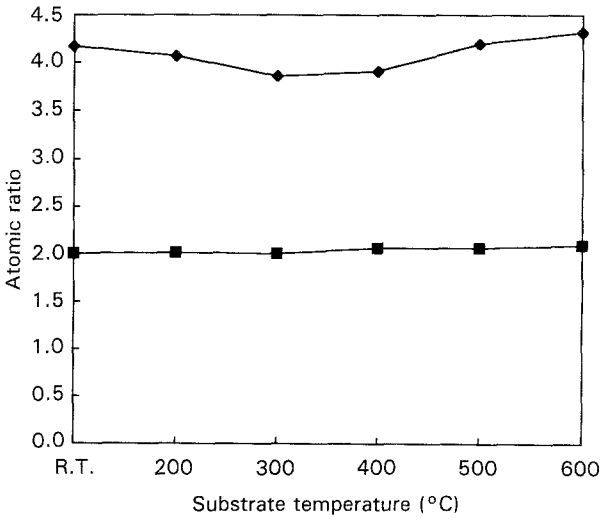

Figure 6 Dependence of atomic ratios (◆) Cu/Y and (■) Ba/Y on the substrate temperatures.

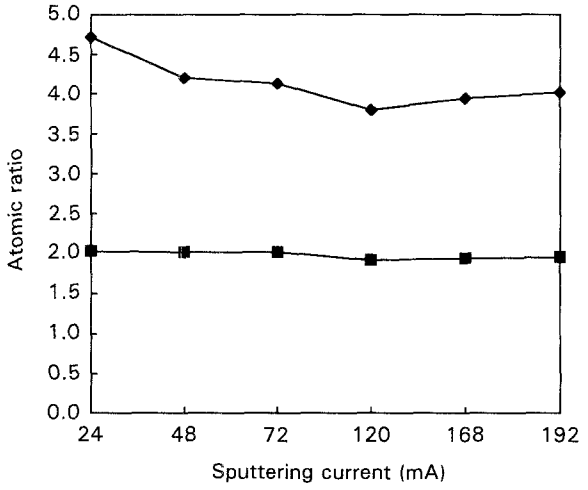

Figure 5 Dependence of atomic ratios (◆) Cu/Y and (■) Ba/Y on the output sputtering current.

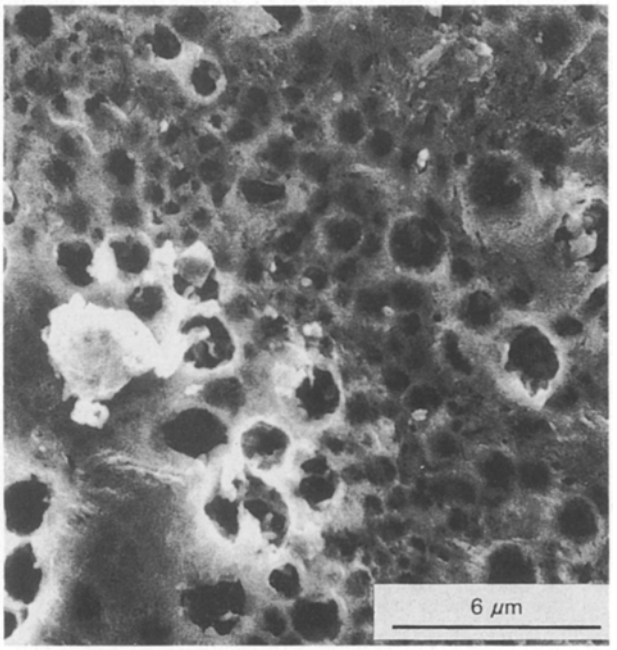

Figure 7 Scanning electron micrograph of the surface of the film, indicating damage caused by resputtering of negative oxygen ions.

coefficient value of each sputtered atom. A detailed study of this will be carried out in the future.

Fig. 8 shows an XRD pattern of the post-annealed film which was deposited under conditions of 500 °C substrate temperature, 300 mtorr chamber pressure, 48 mA output current and 5/100 O_2/Ar ratio. From this XRD pattern, we find that the film exhibits mostly polycrystalline characteristics, with a lower intensity of peak value and no preferred orientation of the *c*-axis; thus, the number of grain boundaries is too large to support the effective electric percolative path transporting current with no resistance and quickly reaching zero-resistive state on cooling the film below the

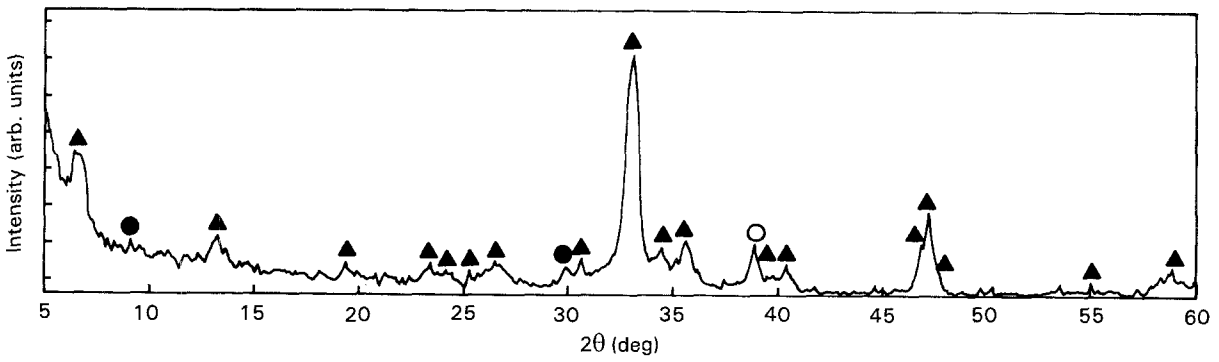

Figure 8 XRD pattern of an annealed film deposited at T_S = 500 °C, O_2/Ar = 5/100, I_{out} = 48 mA, P_{tot} = 300 mtorr. (▲) 124, (○) 123, (●) 211.

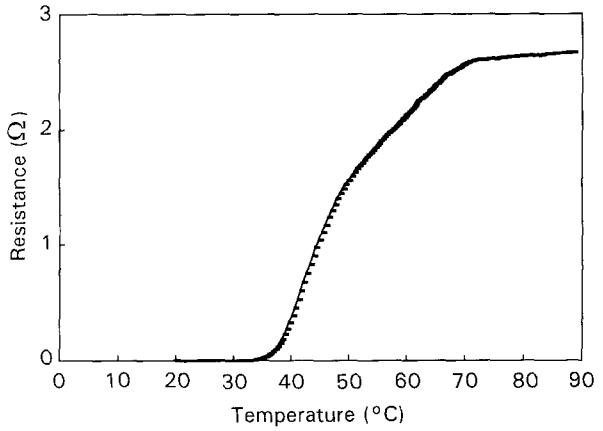

Figure 9 Resistance–temperature curve of post-annealed 124 thin film.

onset temperature. The onset temperature of this film is 75 K, but the point of zero resistivity is at 35 K, as shown in Fig. 9. Probable reasons for the low zero-resistivity temperature are insufficient crystallization and not enough oxygenization during the post-annealing processing.

4. Conclusions

$YBa_2Cu_4O_8$ thin films were deposited by d.c. magnetron sputtering from a single target. An empirical formula, $R = KP^{-a}$, has been proposed on the basis of analysis of the experimental data. It was found experimentally that the degree of dependence of deposition rate of the yttrium atom is the highest of the three atoms, because $a_Y > a_{Cu} > a_{Ba}$. As-deposited films obtained at 500 °C, 300 mtorr, 48 mA and 5/100 O_2/Ar ratio, could transform into a 124 phase on annealing at 800 °C. Owing to insufficient crystallization and not enough oxygenization, the peak density of the XRD pattern of post-annealed films showed weakly, and the zero-resistivity temperature of the film with nearly pure 124 phase was as low as 35 K. It is suggested that accommodating stoichiometric composition of as-deposited film from prediction of the empirical formula and careful consideration of the substrate temperature, output plasma power and oxygen partial pressure, would be an effective means of obtaining a more accurate and general formula to express the results of sputtering growth.

Acknowledgements

One of the authors (H.T.H) thanks R. J. Cheng for assistance with this work. This study was supported by the National Science Council, Taiwan, under project NSC-811-0212-M009-518.

References

1. P. MARSH, R. M. FLEMING, M. L. MANDICH, A. M. DeSANTOLO, J. KWO, M. HONG and L. J. MARTINEZ-MIRANDA, *Nature* **141** (1988) 338.
2. T. MIYATAKE, S. GOTOH, N. KOSHIZUKA and S. TANAKA, *ibid.* **41** (1989) 341.
3. K. YVON and M. FRANCOIS, *Phys. B* **76** (1989) 413.
4. H. W. ZANBERGEN, R. GRONSKY, K. WANG and G. THOMAS, *Nature* **331** (1988) 596.
5. T. KONGURE, R. KONTRA, G. J. YUREK and J. B. VANDER SANDS, *Phys. C* **45** (1988) 156.
6. A. F. MARSHALL, R. W. BARTON, K. CHAR, A. KAPITULUIK, B. OH and R. H. HAMMOND, *Phys. Rev. B* **37** (1988) 9353.
7. M. L. MANDICH, A. M. DeSANTOLO, R. M. FLEMING, P. MARSH, S. NAKAHARA, S. SUNSHINE, J. KWO, M. HONG T. BOONE and T. Y. KOMETANI, *Phys. Rev.B* **38** (1988) 5031.
8. J. KARPINSKI, E. KALDIS, E. JILEK, S. RUSIECKI and B. BUCHER, *Nature* **336** (1988) 600.
9. K. KURODA, K. KOJIMA, M. TANIOKU, K. YOKAYAMA and K. HAMANKA, *Jpn J. Appl. Phys.* **29** (1990) 1439.
10. P. GUPTASARMA, V. R. PALKAR, M. S. MULTANI, R. VIJAYARAGHAVAN, S. T. BENDRE and S. B. OGALE, *Solid State Commun.* **79** (1991) 851.
11. H. HAYASKI, T. SUGIMOTO, K. KIKUCHI, S. YUKYA, Y. YAMADA, M. YOSHIDA, K. SUGAWARA and Y. SHIOHARA, in "Advances in Superconductivity II," edited by T. Ishiguro and K. Kajimura (Springer-Verlag, New York, 1989), p. 431.
12. J. C. HELMER and C. E. WICKERSHAM, *J. Vac. Sci. Technol.* **A4** (1986) 408
13. S. M. ROSSNAGEL, I. YANG and J. J. CROMO, *Thin Solid Films* **59** (1991) 199.
14. W. D. WESTWOOD, *J. Vac. Technol.* **15** (1978) 1.
15. B. CHAPMAN, "Glow Discharge Process" (Wiley-Interscience, New York, 1980) p. 181.
16. T. ARIKAWA, H. ITOZAKI, K. HARADA, K. HIGAKI, S. TANAKA and S. YAZU, *Jpn. J. Apply. Phys.* **29** (1990) 2199.
17. D. J. KESTER and R. MESSIER, *J. Vac. Sci. Technol.* **A4** (1986) 496.
18. J. J. HANAK and J. P. PELLICANE, *ibid.* **13** (1976) 406.
19. J. J. CUOMO, R. J. GAMBINO, J. M. E. HARPER, J. D. KUPTSIS and J. C. WEBBER, *ibid.* **15** (1978) 281.
20. R. E. SOMEKH, *ibid.* **A2** (1984) 1285.

Received 9 November 1993
and accepted 16 May 1994